

M. Sobha¹R. Sreerama kumar²Saly George³

Regular paper

ANFIS based UPFC supplementary controller for damping low frequency oscillations in power systems

An adaptive neuro-fuzzy inference system (ANFIS) based supplementary Unified Power Flow Controller (UPFC) to superimpose the damping function on the control signal of UPFC is proposed. By using a hybrid learning procedure, the proposed ANFIS construct an input-output mapping based on stipulated input-output data pairs. The linguistic rules, considering the dependence of the plant output on the controlling signal are used to build the initial fuzzy inference structure. On the basis of linearized Philips-Hefron model of power system installed with UPFC, the damping function of the UPFC with various alternative UPFC control signals are investigated. In the simulations under widely varying operating conditions and system parameters, ANFIS based controller yields improved performance when compared with constant gain controller, based on phase compensation technique. To validate the robustness of the proposed technique, the approach is integrated to a multi-machine power system and the non-linear simulation results are presented.

Keywords ANFIS, UPFC, Fuzzy logic, low frequency oscillations, Power system stability

1. INTRODUCTION

With the development of interconnection of large electric power systems there have been spontaneous system oscillations at low frequencies in the order of several cycles per minute. These low frequency oscillations are predominantly due to the lack of damping of mechanical mode of the system. Since power oscillation is a sustained dynamic event, it is necessary to vary the applied compensation to counteract the accelerating and decelerating swings of the disturbed machine [1]. The concept of Flexible AC transmission system (FACTS) envisages the use of solid state controllers to achieve flexibility of power system by fast and reliable control of power system parameters affecting power flow in transmission line, namely voltage, impedance and or phase angle [2]. Unified Power Flow Controller (UPFC), a multifunctional Flexible AC Transmission system (FACTS) Controller [3] opens up new opportunities for controlling power and enhancing the usable capacity of present, as well as new and upgraded lines.

A UPFC supplementary damping controller has been presented in the UPFC control system [4] for damping the electromechanical mode oscillations. In [5,6] systematic design of four alternative UPFC damping controllers are presented. However, these UPFC damping controller gains are designed on the basis of nominal operating conditions and remain independent of system operating conditions and line loadings. Also the controller gains and hence the control structure is different for the various choices of UPFC control signals. Since damping of low frequency oscillations may be one of the secondary functions of the multifunctional UPFC based on its other major control assignments, the widely varying control structure with respect to the choice of control signals makes the real time

Department of Electrical Engineering, National Institute of Technology Calicut Kerala 673 601, India

1. sobha_kumar1@rediffmail.com, 2. sreeram@nitc.ac.in, 3. saly@nitc.ac.in

implementation inflexible. This work proposes an adaptive fuzzy inference system (ANFIS) based [7] UPFC supplementary damping controller to superimpose the damping function on the control signal of UPFC for damping of power system electromechanical oscillations [8]. The adaptive fuzzy controller is obtained by embedding the fuzzy inference system into the framework of adaptive networks. The proposed ANFIS based damping controller performance is examined for the four choices of UPFC control signals based on modulating index and voltage phase angle of UPFC series and shunt converters by simulations on a linearised Philips-Hefron model of a power system with UPFC [9]. The effectiveness of this controller is supported by the results observed in simulations, which show the ability of the controller in damping oscillations over a wide range of loading conditions and system parameters with the four choices of alternative UPFC control signals when compared to constant gain damping controllers designed using phase compensation technique at selected operating point. Integrating this approach to a multi-machine power system and through non- linear simulation the robustness of the proposed controller is validated.

2. DYNAMIC MODELING OF POWER SYSTEM WITH UPFC

2.1. Single machine infinite bus system installed with UPFC

As shown in Fig.1 the single machine infinite-bus power system installed with a UPFC consists of an excitation transformer (ET), a boosting transformer (BT), and two three phase GTO based voltage source converters and DC link capacitor. Pulse width modulation is assumed for the UPFC series converter VSC-B and shunt converter VSC-E.

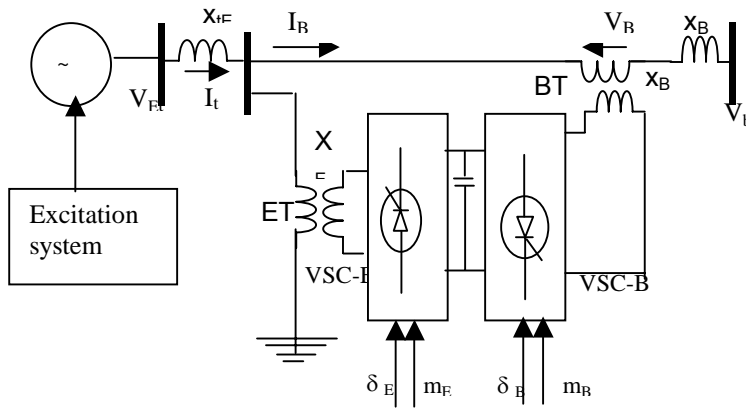


Fig.1 SMIB System with UPFC

The excitation system is considered to be of type IEEE-ST1A[13]. In the figure, m_E : modulating index of shunt converter, m_B : modulating index of series converter, δ_E : phase angle of shunt converter voltage and δ_B : phase angle of series converter voltage are the input control signals to the UPFC. The three phase differential equations representing the dynamics of UPFC neglecting the transformer resistances and transients are given by [9,11]

$$V_B = \begin{pmatrix} m_B v_{dc/2} \end{pmatrix} e^{j\delta_B} \quad V_b = \begin{pmatrix} m_B v_{dc/2} \end{pmatrix} e^{j\delta_B} \quad (2.1)$$

$$\dot{v}_{dc} = 3 m_E/4 \begin{bmatrix} \cos \delta_E & \sin \delta_E \end{bmatrix} \left[\begin{bmatrix} \dot{i}_{Ea} \\ \dot{i}_{Eb} \end{bmatrix} \right] + 3 m_B/4 \begin{bmatrix} \cos \delta_B & \sin \delta_B \end{bmatrix} \left[\begin{bmatrix} \dot{i}_{Ba} \\ \dot{i}_{Bb} \end{bmatrix} \right] \quad (2.2)$$

Here m_E , δ_E , m_B , δ_B are the UPFC control signals, C_{dc} the steady state capacitance of the dc link, i_E , and i_B the UPFC currents.

The overall model of the generator, exciter and the power system with UPFC are given by

$$\dot{x}(t) = f(x(t), u(t)) \quad (2.3)$$

$x(t)$ represents the state vector given by

$$x(t) = \begin{bmatrix} \delta & \omega & E_q' & E_{fd} & v_{dc} \end{bmatrix} \quad (2.4)$$

$u(t)$ represents the control vector given by

$$u(t) = \begin{bmatrix} m_E & m_B & \delta_E & \delta_B \end{bmatrix} \quad (2.5)$$

The linearized model of equations (2.3),(2.4) and (2.5) is given by equation (2.6)

$$\begin{bmatrix} \dot{\Delta\delta} \\ \dot{\Delta\omega} \\ \dot{\Delta E_q'} \\ \dot{\Delta E_{fd}} \\ \dot{\Delta v_{dc}} \end{bmatrix} = \begin{bmatrix} 0 & \omega_0 & 0 & 0 & 0 \\ -K_1/M & -D/M & -K_2/M & 0 & -K_{pd}/M \\ -K_4/T'_{do} & 0 & -K_3/T'_{do} & 1/T'_{do} & -K_{qd}/T'_{do} \\ -K_A K_5/T_A & 0 & -K_A K_6/T_A & -1/T_A & -K_A K_{vd}/T_A \\ K_7 & 0 & K_8 & 0 & -K_9 \end{bmatrix} \times \begin{bmatrix} \Delta\delta \\ \Delta\omega \\ \Delta E_q' \\ \Delta E_{fd} \\ \Delta v_{dc} \end{bmatrix} \\ + \begin{bmatrix} 0 & 0 & 0 & 0 \\ -K_{pe}/M & -K_{pde}/M & -K_{pb}/M & -K_{pdb}/M \\ -K_{qe}/T'_{do} & -K_{qde}/T'_{do} & -K_{qb}/T'_{do} & -K_{qdb}/T'_{do} \\ -K_A K_{ve}/T_A & -K_A K_{vde}/T_A & -K_A K_{vb}/T_A & -K_A K_{vdb}/T_A \\ K_{ce} & K_{cde} & K_{cb} & K_{cdb} \end{bmatrix} \times \begin{bmatrix} \Delta m_E \\ \Delta \delta_E \\ \Delta m_B \\ \Delta \delta_B \end{bmatrix} \quad (2.6)$$

2.2. Multi-machine system with UPFC

In Fig.2, the generators and the line with UPFC are shown to be connected to the network with the bus admittance $[Y_1]$, which represents the power system admittance excluding the UPFC part and the admittance matrix is further modified to account for these impedances.

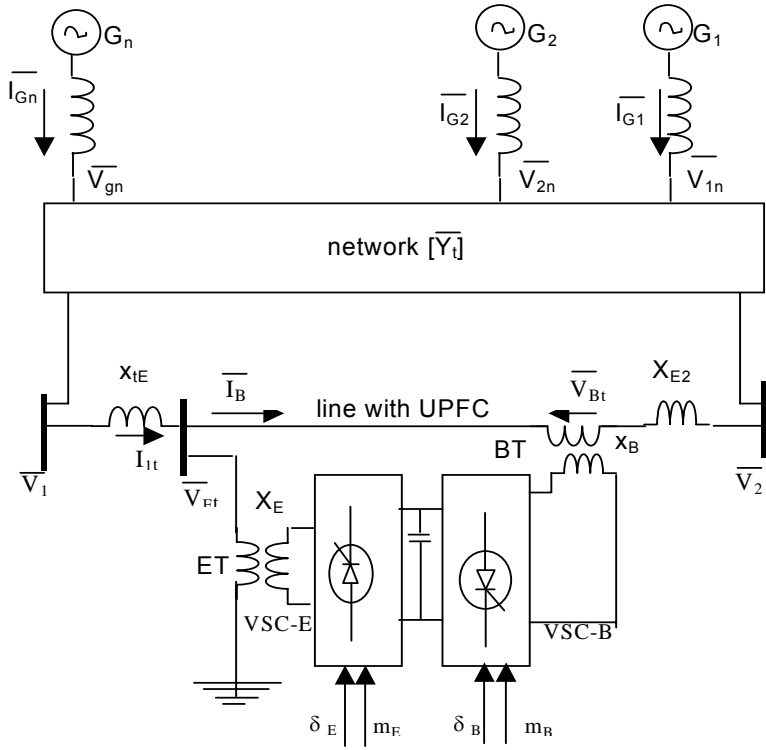


Fig. 2. Multi-machine power system with UPFC

The equations representing the dynamics of the power system with UPFC [12] are given

by

$$\dot{\delta} = \omega_0 (\omega - 1) \quad (2.7)$$

$$\dot{\omega} = M^{-1} (P_M - P_e - D\omega) \quad (2.8)$$

$$\dot{E}'_q = T'_{do} \left((X_X - X'_D)I_d - E'_q + E_{fd} \right) \quad (2.9)$$

$$\dot{E}'_{fd} = -T_A^{-1} E_{fd} + T_A^{-1} K_A (V_{ref} - V_T) \quad (2.10)$$

$$\dot{v}_{dc} = 3 m_E/4 \left[\cos \delta_E \sin \delta_E \right] \left[\begin{matrix} \dot{i}_{Ed} \\ \dot{i}_{Eq} \end{matrix} \right] + 3 m_B/4 \left[\cos \delta_B \sin \delta_B \right] \left[\begin{matrix} \dot{i}_{Bd} \\ \dot{i}_{Bq} \end{matrix} \right] \quad (2.11)$$

Here,

$$\delta = [\delta_1 \delta_2 \dots \delta_n]^T, \omega = [\omega_1 \omega_2 \dots \omega_n]^T, E_q' = [E_q'1 E_q'2 \dots E_q'n]^T$$

$$E_{fd} = [E_{fd1} E_{fd2} \dots E_{fdn}]^T, I_d = [I_{d1} I_{d2} \dots I_{dn}]^T, V_T = [V_{T1} V_{T2} \dots V_{Tn}]^T$$

$$M = \text{diag}(M_i), D = \text{diag}(D_i), T'_{do} = \text{diag}(T'_{do_i}), X_D = \text{diag}(X_{D_i}), X'_D = \text{Diag}(X'_{D_i}), X_Q = \text{Diag}(X_{Q_i})$$

3. CONSTANT GAIN DAMPING CONTROLLER FOR UPFC

The UPFC is installed for the purpose of multiple control functions, one of which will be the suppression of low-frequency oscillations occurring in the system. In literature [3-6] the effectiveness of improving the oscillation damping by a FACTS supplementary damping controller has been explored. Various feedback signals namely, deviation in generator rotor angle, deviations in real power flow through the transmission line, accelerating power, have been identified as capable of contributing direct electric damping torque to the electromechanical oscillation loop of the generator. The selection criteria chosen in these works consider the control cost, robustness of the feedback signal to variations of system operating conditions and local availability of signal. A judicious selection of the feed back signal can be done based on its capability in improving the damping of desired mode of oscillation. This work considers the deviation in rotor angle as input signal for the single machine infinite bus system aiming at improving the local mode of oscillation and the locally available power flow through the transmission line at which UPFC is connected, aiming at improving the poorly damped oscillation mode for the case of multi-machine.

Thus these signals are capable of generating efficient database for the training of adaptive controller.

3.1. Single machine infinite bus system

A supplementary damping controller as shown in Fig.(3) which consists of gain, signal washout and phase compensator circuits is installed in the SMIB system represented by eqt(2.6) to superimpose the damping function on the UPFC control signal. The input to the controller is $\Delta\omega$, the deviation in the generator angular speed and the output is Δu , the damping control signal. The system parameters and the k values calculated for the nominal operating condition is given in Appendix 1.

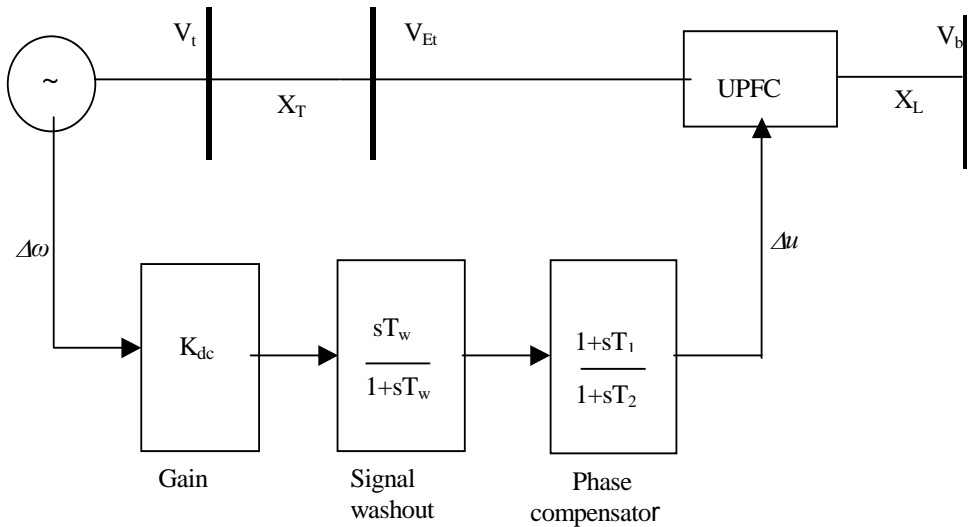


Fig.3.. System installed with UPFC and the complementary damping

It is observed that the system is having an oscillatory mode $\lambda = 0.0122 \pm 4.0935i$ in the mechanical loop which is desired to be improved by introducing an electrical torque in phase with speed deviation. The gain settings and time constants for the damping controller

are calculated by phase compensation technique [10]. The value of the washout time constant, T_w is taken as 10 secs. The controller is designed for the four alternative choices of UPFC control signals namely, modulating index of series converter (m_B), modulating index of shunt converter (m_E), phase angles of series converter voltage (δ_B) and phase angles of shunt converter voltage (δ_E). Table .1 shows the improvement in damping produced for the various choices of control signals. The corresponding parameters of the UPFC damping controllers designed are as shown in Table2.

Table 2 indicates that the control parameters, for the four choices of UPFC control signals have widely varying gain constants based on the conventional design. This essentially makes the hardware implementation difficult when the system demands for different control signals so as to exploit the multifunctional capability of the installed UPFC. This motivates the need for having an adaptive controller, which gives freedom for the selection of UPFC control signal based on its other functions. The proposed ANFIS based adaptive controller is given in section 4.

Table1.Eigen values with the various UPFC control signals

$\Delta\delta_B$	$\Delta\delta_E$	Δm_E	Δm_B
-92.5572	-92.7281	-92.6118	-92.6118
$-2.7947 \pm 7.4102i^a$	$-2.9553 \pm 8.3846i^a$	$-1.0481 \pm 7.8108i^a$	$-1.0481 \pm 7.8108i^a$
-8.6269	-7.6317	-8.0652	-8.0652
-0.1016	-0.1007	-0.1020	-0.1020

^a electromechanical mode

Table.2 Parameters of constant gain UPFC damping controllers

Controller parameters UPFC Control signal	K_{dc}	$T_1(s)$	$T_2(s)$
m_E	95.1	0.16	0.235
δ_E	33.1	0.20	0.18
m_B	211.1	0.172	0.218
δ_B	336	0.204	0.183

3.2. Multi-machine system

A 3-machine 9-bus system as shown in Fig.4 is considered by incorporating a UPFC in the line 7-8. The system with UPFC is represented by the non-linear equations (2.7) to (2.11). Excitation system is considered for all machines and machines 2 & 3 are assumed to be provided with power system stabilizers. The system data are given in Appenix2.A.The UPFC ratings are so chosen to enhance the power flow through the line 7-8 by 10% along with sufficient transient and design margin [3]. The steady state values for the UPFC series

and shunt voltages computed by modifying the load flow with the UPFC are given in Appendix 2.(B).

The system simulation indicate the presence of slightly negatively damped mode of oscillation with $\lambda = 0.0003 \pm 5.7150i$, responsible for a low frequency oscillation of around 0.9 Hz in the system. The supplementary damping controller is designed targeting at improving the damping of this mode. The feed back signal is chosen as deviation in power flow in the line 7-8 which can be locally measured. Modulation of the phase angles of series converter voltage (δ_B) is identified as the most significant UPFC control signal for damping this mode of oscillation [10]. The parameters of the supplementary damping controller with δ_B computed for the nominal operating condition using the multi-modal decomposition and phase compensation technique [8, 10] are given in Appendix 2.(B).

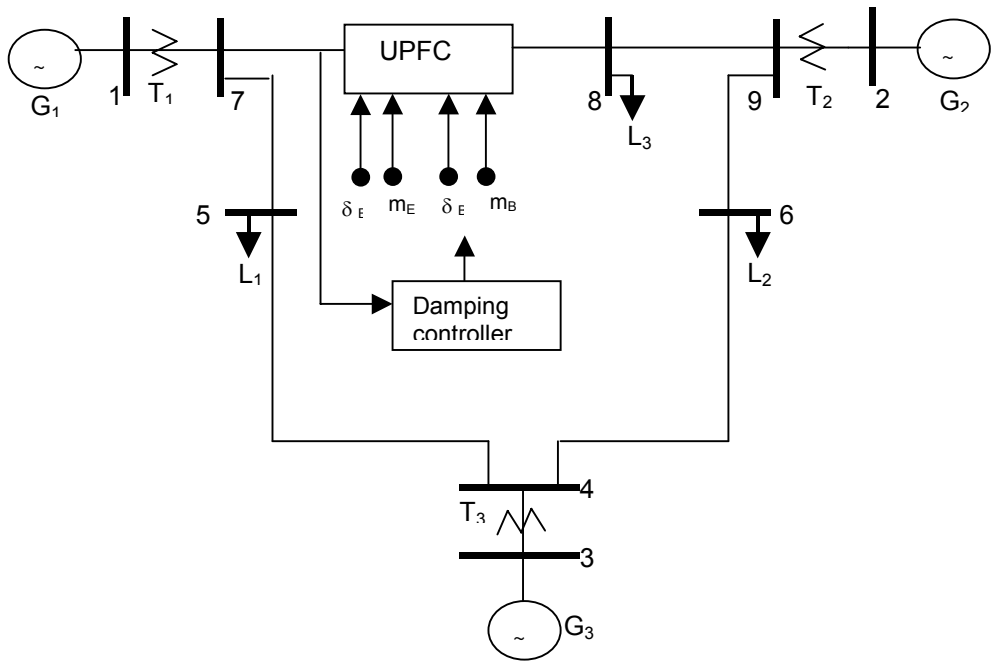


Fig. 4. 3-Machine, 9-Bus system installed with UPFC

4. ADAPTIVE FUZZY DAMPING CONTROLLER FOR UPFC

To maintain good dynamic response at various operating conditions with the four possible choices of UPFC control signal, the controller gains need to be adapted based on system conditions. An adaptive fuzzy inference system has been used in this work to adapt the controller gains of UPFC damping controller. The steps involving the passage from classical fuzzy logic to the neuro-adaptive learning approach is briefly presented here.

- Determination of initial fuzzy structure.
- ANFIS training of the initial fuzzy structure for updating the fuzzy parameters to meet the desired control performance.
- Evaluation of the performance of the ANFIS controller under different operating situations.

The various steps involved are elaborated with reference to UPFC installed in SMIB system

4.1. Determination of initial fuzzy structure

The input to the proposed fuzzy inference system is taken as the deviation in the generator angular speed ($\Delta\omega$), and the output as the damping control signal, (Δu) same as in the case of constant gain controller. The linguistic rules, considering the dependence of the plant output on the controlling signal, are used to build the initial fuzzy inference structure. An increasing trend in speed deviation results in excess accelerating power and the control action should be in such a way to promote the power flow to maintain the power balance and vice-versa.

The input signal is fuzzified using seven fuzzy sets A_i ; $i=1$ to 7. Any continuous and piecewise differentiable functions are qualified candidates for node functions of premise parameters of the ANFIS structure. However to satisfy the Stone-Weierstrass theorem [7] it is desirable that the class of membership function is invariant under multiplication. This work considers the generalized bell-shaped function as the initial fuzzy membership function, with maximum equal to 1 and minimum equal to 0 and is given by

$$\mu_{A_i}(X) = 1 / 1 + [(X - c_i) / a_i]^2]^{b_i} \quad (4.1)$$

where $\{a_i, b_i, c_i\}$ is the *premise parameter set*. The initial values of premise parameters are set in such a way that the MF's are equally spaced in the range [-1 1]. The rule base with seven fuzzy if-then rules of (TS) Takagi and Sugeno's type [14] given by

$$\text{If } \Delta\omega_i \text{ is } A_i \text{ then } \Delta u_i \text{ is } p_i x + r_i; i=1 \text{ to } 7 \quad (4.2)$$

Table 3. Initial premise and consequent parameters

Parameters ↓ MF's →	a_i	b_i	c_i	p_i	r_i
A_1	0.1667	2.5	-1	0	0
A_2	0.1667	2.5	-0.6666	0	0.1666
A_3	0.1667	2.5	-0.3334	0	0.3333
A_4	0.1667	2.5	0	0	0.5
A_5	0.1667	2.5	0.3334	0	0.6666
A_6	0.1667	2.5	0.6666	0	0.8333
A_7	0.1667	2.5	1	0	1

The output Δu , the output control signal of the damping controller is calculated by the linear combination of the inputs and $\{p_i, r_i\}$ denote the *consequent parameter set*. Table 3. shows the premise parameters initially chosen and the resulting consequent parameters generated based on the rule base and membership function. These parameters are updated

by ANFIS training process presented in section 4.2. However the seven rules of the initial fuzzy structure remain unchanged during the adaptation process.

4.2. ANFIS training

The steps for ANFIS training to adapt the initial fuzzy premise parameters for construction of the proposed optimum input output pattern to perform the desired control action at various operating conditions is presented.

i) Selection of the network architecture

A four layer feed forward network architecture is selected for the ANFIS based damping controller as shown in Fig.5. The node functions of the various layers of ANFIS for the adjustments of premise parameter set $\{a_i, b_i, c_i\}$ are as follows.

Layer 1: This layer has adaptive nodes denoted by squares with node function

$$O_i^1 = \mu_{A_i}(X) ; i = 1 \text{ to } 7 \quad (4.3)$$

where X is the input to node i , A_i the linguistic label associated with this node. O_i specify the degree to which the given X satisfies the quantifier A_i . Parameters in this layer are referred to as *premise parameters* is denoted by the parameter set $\{a_i, b_i, c_i\}$

Layer 2: Every node in this layer is fixed, denoted by circle, which calculates the ratio of the i^{th} rule's firing strength to the sum of all rules' firing strengths

$$\bar{\omega}_i = \omega_i / \sum \omega_i ; i = 1 \text{ to } 7 \quad (4.4)$$

where ω_i represents the firing strengths of each rule and $\bar{\omega}_i$ the *normalized firing strengths* for the output function.

Layer 3: This adaptive node layer represented by squares has a node function

$$O_i^3 = \bar{\omega}_i f_i = \bar{\omega}_i (p_i X + r_i) ; i = 1 \text{ to } 7 \quad (4.5)$$

$\{p_i, r_i\}$ is the parameter set of this adaptive layer and is referred to as *consequent parameters*

Layer 4: The single node in this layer represented by a circle labelled Σ computes the overall output as the summations of all incoming signals

$$O_i^4 = \text{overall output} = \sum \bar{\omega}_i f_i = \sum \bar{\omega}_i (p_i X + r_i) ; i = 1 \text{ to } 7 \quad (4.6)$$

ii). Learning Algorithm

The choice of learning algorithm is based on trade-off between computation complexity and resulting performance. The learning method adopted in this work is the hybrid learning rule combining the learning rule based on the gradient descent method and the Least Square Error (LSE) method [7]. This hybrid learning technique speeds up the learning process compared to the gradient method alone, which exhibits the tendency to become trapped in local minima.

Each epoch of this hybrid learning procedure is composed of a forward pass and backward pass. In the forward pass the training data is presented and the functional signals proceed forward to calculate each node output. The consequent parameters are identified and error measure is calculated. In the backward pass, the error rates propagate from the output end toward input end and the premise parameters are updated by gradient method. The update action on premise parameters takes place only after the whole training data set is presented thus adopting batch learning paradigm for the learning algorithm. Steps to demonstrate the use of the hybrid-learning algorithm for training ANFIS are as follows:

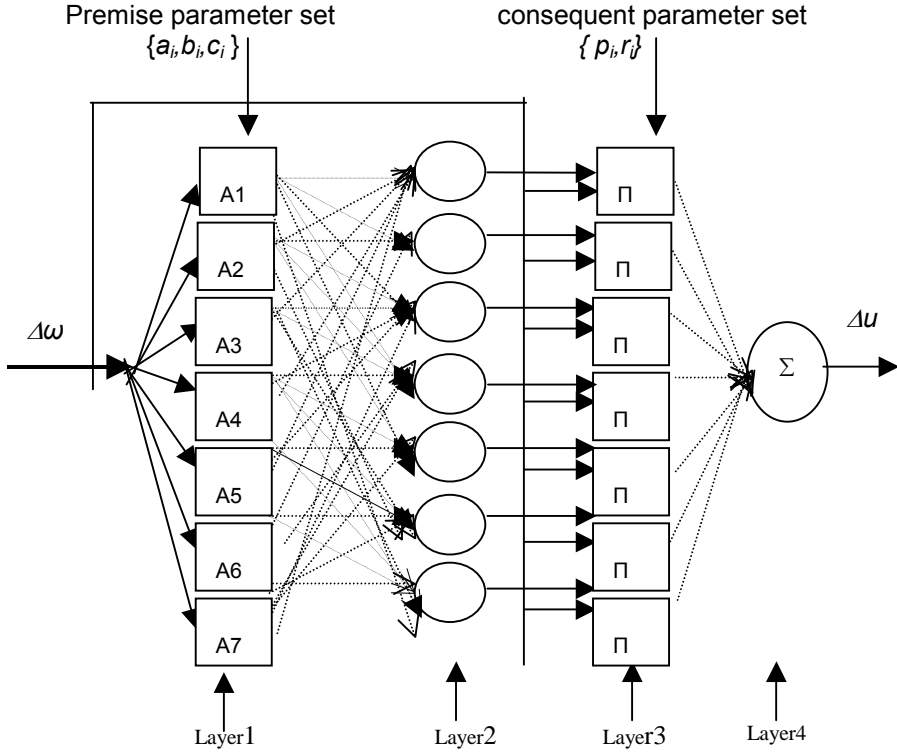


Fig. 5. ANFIS Architecture

a. Initialisation

- Load input vector $[\Delta\omega_j \ \Delta u_j]$; $j=1$ to P , P the number of training pairs used
- Select MF A_i ; $i=1$ to 7
- Initialize premise parameter matrix $\{a_i \ b_i \ c_i\}$ for Generalized Bell membership
 a =half width of bell function, b -slopes at crossover point (where $MF=0.5$),
 c = center of corresponding membership function
- Select SSE goal =0.05; learning rate $\eta=0.5$

b. Forward pass

- Layer 1. Generate membership grades; $A_i = [\Delta\omega_j \ [a_i \ b_i \ c_i]]$
- Layer 2. Generate firing strengths $\omega_i=A_i$; $i=1$ to 7
- Layer3. Normalize firing strengths $\varpi_i = \omega_i / \sum \omega_i$; $i=1$ to 7
- Compute consequent parameters(C_params) , $\{p_i, r_i\}$; $i=1$ to 7 using LSE algorithm
 $\Delta u_{inner} = [\varpi_i \times \Delta\omega_j]$; $i=1$ to 7
 $C_params = ((\Delta u_{inner})^T \times \Delta u_{inner})^{-1} \times (\Delta u_{inner})^T \times \Delta u_j$; $j=1$ to P
- Layer4. Calculate outputs using latest consequent parameters
 $y = [C_params]^T \times \Delta u_{inner}$

c. Backward pass

Estimate error gradient vectors using gradient descent algorithm of hybrid learning rule

- Calculate output error $e = y - \Delta u_j$

- Calculate SSE
- $SSE = \sum (\sum (e)^2)$; If $SSE < SSE_{goal}$ stop training. Else
- Propagate derivative of error measure for each node in the four layers
- Compute $\partial E / \partial [a_i b_i c_i]$, overall error measure with respect to each premise parameter
- Update premise parameters

$$\Delta [a_i b_i c_i] = -\eta \times \partial E / \partial [a_i b_i c_i]$$

$$[a_i b_i c_i]_{new} = [a_i b_i c_i] + \Delta [a_i b_i c_i]$$

iii) Training Data

The proposed fuzzy structure has 21 premise parameters and 14 consequent parameters to be estimated. The data base for the optimum input-output pattern required for the training of the ANFIS is generated as follows.

i. Design constant gain damping controller using phase compensation technique as given in section 3.1. Design is carried out at various combination of loading and network conditions with active power P_e , reactive power Q_e and system equivalent reactance X_e varying in the range given by $\{P_e, Q_e, X_e\} = \{0.1-1.2, 0.01-0.4, 0.3-0.9\}$ (all in per unit).

ii. Repeat step i. for the various choices of UPFC control signals namely $m_E, m_B, \delta_E, \delta_B$

iii. Generate $(\Delta\omega, \Delta u)$ training pairs from the constant gain controller so designed.

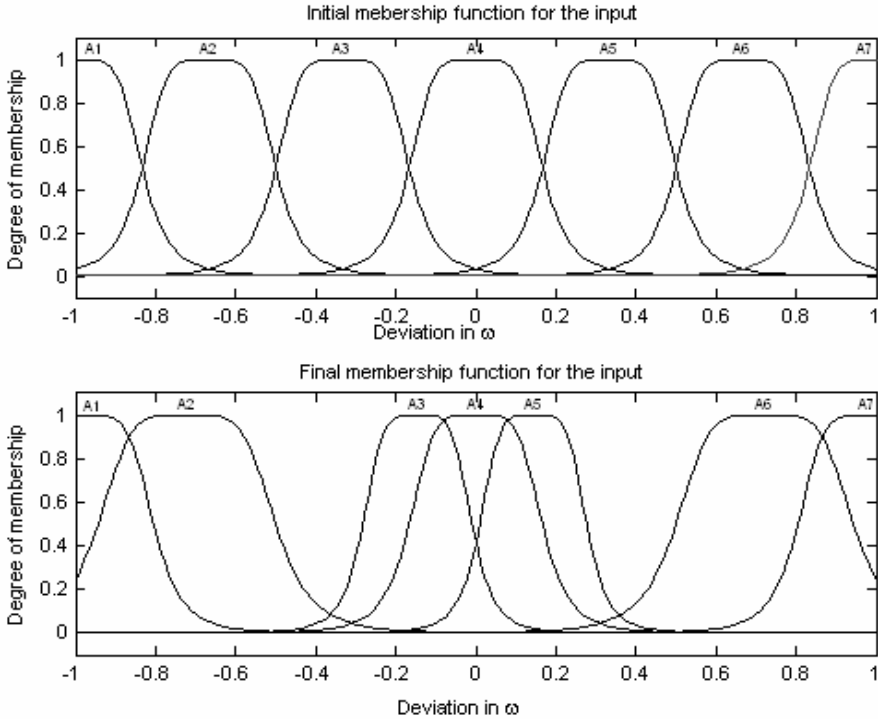


Fig.6. Membership functions prior to and after ANFIS training

The adaptive network is trained using the training data generated and the hybrid-learning algorithm. The distribution of initial fuzzy subset of the seven MF's (A_1 to A_7) in the universe of discourse of input function $\Delta\omega$ is equally spaced in the range $[-1, 1]$. The membership functions of the resulting fuzzy inference system after 40 training epochs

when the error reduced to 0.0404 is shown in Fig.6.From the figure it can be seen that the membership functions have moved towards the origin and these changes are more for the middle membership functions due to the sharper changes of the training data around the origin. The corresponding premise and the consequent parameters are given in Table4.

Table .4 Final premise and consequent parameters

Parameters ↓ MF's	a_i	b_i	c_i	p_i	r_i
A ₁	0.1721	2.5005	-0.976	-2.22	-2.131
A ₂	0.2222	2.5008	-0.7218	-0.150	3.634
A ₃	0.1360	2.5181	-0.1458	3.107	-2.94
A ₄	0.1667	2.4999	-0.7379	4.550	-0.383
A ₅	0.1336	2.5184	0.4328	3.142	3.971
A ₆	0.2222	2.5008	0.7218	-0.150	-3.633
A ₇	0.1721	2.5005	0.9769	-2.223	2.132

4.3. Performance evaluation of the of the ANFIS controller

The final step of adaptive controller design is the performance evaluation of the controller under varying operating condition, network configuration and with the various choices of control signals. This is done by time domain simulation of the system given in Fig. (1) and Fig. (4) with the proposed ANFIS controller using the MATLAB/SIMULINK toolboxes. The simulation results are presented and discussed briefly in Secion.5.

5. SIMULATION RESULTS

Investigations are carried out on the system shown in Fig.1 and is repeated for each of the UPFC control signal namely m_E , m_B , δ_E and δ_B under various operating conditions. Non-linear simulation is performed on the system shown in Fig.4. to validate the controller performance under large disturbance. The following cases are considered.

Case(A) Small signal analysis on SMIB system

i) Step change in Mechanical Power input

Fig.7 shows the variation of $\Delta\omega$ of the synchronous machine in the system shown in Fig.1 for a step rise of 0.01p.u in the mechanical power input of the machine at the time instant t=0.5 second when the machine is operating in the nominal operating conditions as listed in Appendix.1. The UPFC control signals considered in Fig.7. a to Fig.7.d are m_E , m_B , δ_E and δ_B respectively. From these figures it is evident that the system becomes unstable whatever be the UPFC control signal, if the UPFC is not provided with a supplementary damping controller.

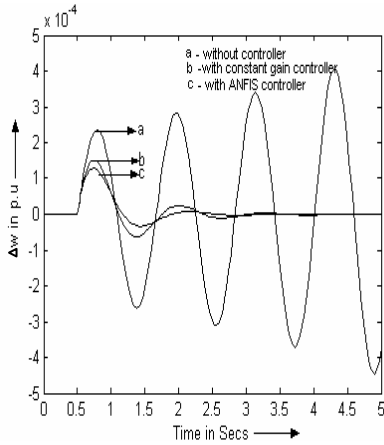


Fig.7 (a). variation of $\Delta\omega$ for step change in mech. input ;UPFC control signal m_E

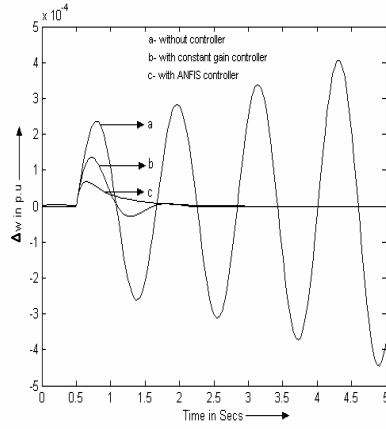


Fig.7 (b). variation of $\Delta\omega$ for step change in mech. input ;UPFC control signal m_B

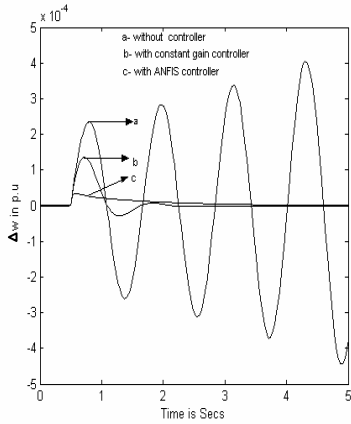


Fig.7(c). variation of $\Delta\omega$ for step change in mech. input ;UPFC control signal δ_E

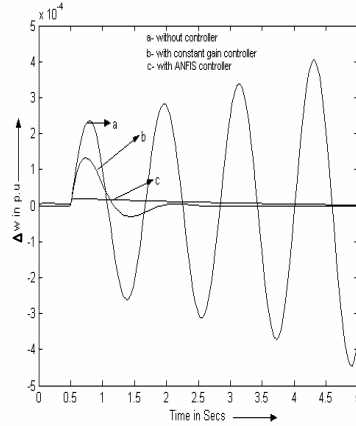


Fig.7 (d). variation of $\Delta\omega$ for step change in mech. input ;UPFC control signal δ_B

Further it can be seen that the proposed ANFIS based UPFC supplementary damping controller shows better damping performance when compared to that with constant gain controller for these control signals. Fig.7.e shows the effect of the UPFC control signals m_E , m_B , δ_E and δ_B on the system performance when the UPFC is provided with the proposed ANFIS controller. It is observed that the peak overshoot is minimum when the UPFC control signals are δ_E & δ_B namely, the phase angle of the shunt and series converter. This is in confirmation with the eigen value results presented in Table 1 from which these signals are found to be contributing more towards damping of the concerned mode. This can be attributed to the fact that modulation in δ_E & δ_B results in exchange of real power with the system. Thus further analyses are done with respect to these signals.

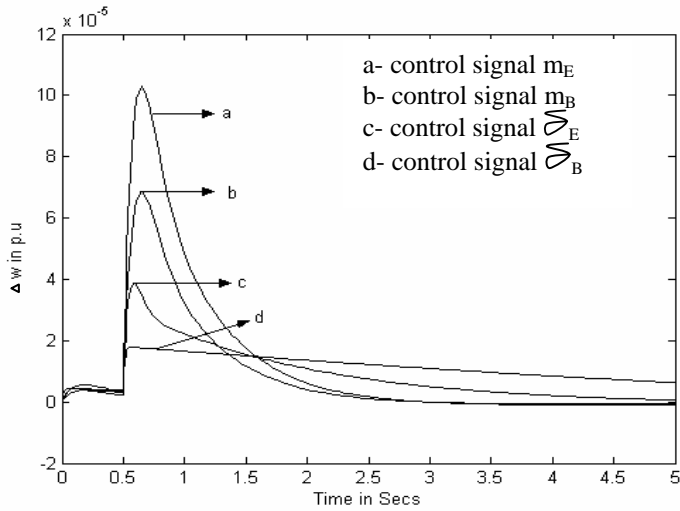


Fig.7(e) variation of $\Delta\omega$ for step change in mech. input for four UPFC control signals

ii) Changes in system loading

To examine the robustness of the damping controllers with the more significant control signals namely δ_E & δ_B to variation in system loading, simulation studies are done on the system given in Fig.1, varying the active power P_e and reactive power Q_e in the range given by $P_e : 0.1p.u$ to $1.2 p.u$, $Q_e : 0.01p.u$ to $0.4 p.u$. Fig.8 shows the variation of $\Delta\omega$ of the synchronous machine in the system shown in Fig.1 for a step rise of $0.01p.u$ in the mechanical power input of the machine at the time instant $t=0.5$ second when the machine is operating with loading conditions active and reactive power flows above the nominal operating conditions. It is evident that the proposed adaptive controller is exhibiting superior performance when compared to the constant gain controller for the various UPFC control signals considered. Similar results are obtained when the machine is operating with loading conditions, active and reactive power flows below the nominal operating conditions.

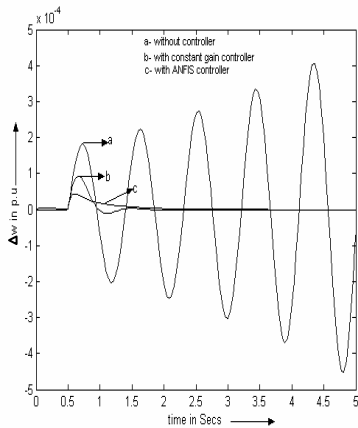


Fig.8 (a). variation of $\Delta\omega$ for step change in mech. input ; $P_e=1.2p.u$; $Q_e=0.4p.u$. (UPFC control signal δ_E)

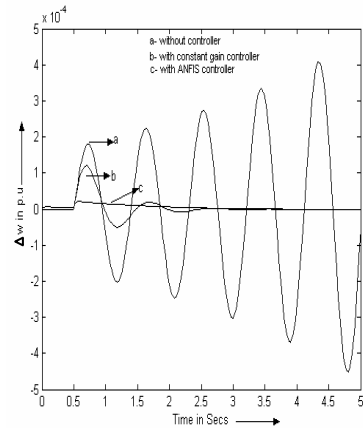


Fig.8 (b). variation of $\Delta\omega$ for step change in mech. input ; $P_e=1.2p.u$; $Q_e=0.4p.u$. (UPFC control signal δ_B)

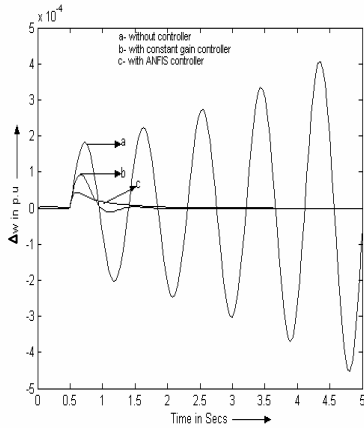


Fig.9 (a) .variation of $\Delta\omega$ for step change in mech. input ; $X_e = 0.9 p.u.$ (UPFC control signal δ_E)

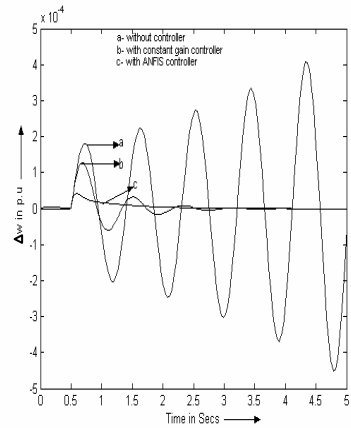


Fig.9 (b). variation of $\Delta\omega$ for step change in mech. input ; $X_e = 0.9 p.u.$ (UPFC control signal δ_B)

iii) Changes in network conditions

Under a faulty condition or while switching transmission lines, the line reactance will change in the order of 0.3 pu to 0.9 pu. The performance of the damping controllers with the chosen control signals is further analyzed with variation in equivalent reactance, X_e of the system in this range and results pertaining to a value of X_e higher than nominal, are presented in Fig.9. Similar results are obtained with lower value of X_e . Examining the simulation results it can be inferred that the proposed controller is quite robust to variation in X_e and exhibiting superior performance when compared to constant gain controller for the UPFC control signals considered.

Case(B). Non-linear simulation on multi-machine system

i) Machines at nominal operating condition

The system shown in Fig.4 is assumed to be operating at the nominal load condition at which the supplementary controller design with the chosen control signal, namely δ_B is done. The loading and system conditions are given in Appendix2. The oscillation is triggered by a three-phase short circuit occurring at the machine terminal G2 at 1.0 second of the simulation and cleared after 100 ms. Fig.10 show the comparison of the variation of relative rotor angle of G2 with respect to G1 when the system is equipped with the constant gain controller and the proposed ANFIS based adaptive controller whose gains have been adapted with respect to various system conditions. It is observed that the performance of both the controllers are almost similar except for the lesser settling time in the case of ANFIS based controller. The simulation is repeated by increasing the clearing time to 120 ms and the results are presented in Fig.11 (a) & Fig.11.(b). It is evident that with the constant gain controller, machine G2 shows signs of instability with the drifting of rotor angle where as with the proposed controller the machines are swinging together.

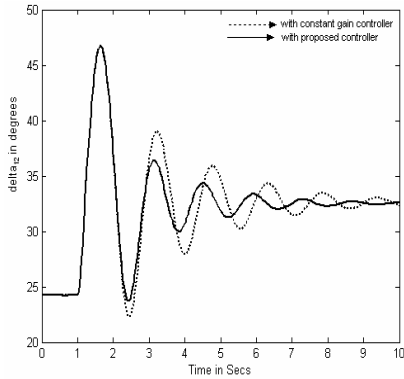


Fig.10. Nominal operating condition (fault cleared at 100ms)

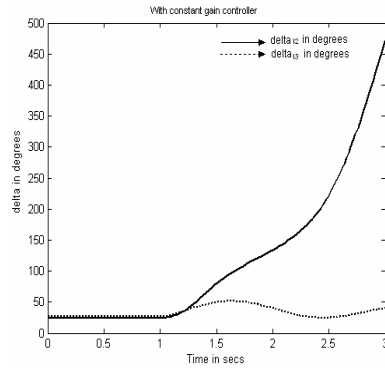


Fig.11(a). Fault cleared at 120 ms (with constant gain controller)

ii) Machines at higher than nominal operating condition

The machines are assumed to be operating at a condition, above the nominal load condition at which the controller design has been carried out. The loading condition with respect to this operating point is given in Appendix 2(A). The oscillation is triggered by a three-phase short circuit occurring at the machine terminal G2 at 1.0 second of the simulation and cleared after 100ms. Fig.12 compares the performance of the constant and the proposed controllers at this condition. It is observed that the proposed controller performance is superior showing lesser over shoot and is less oscillatory compared to the constant gain controller.

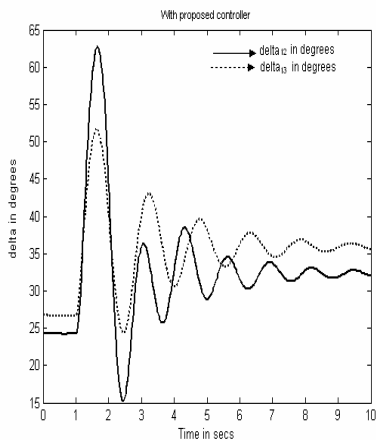


Fig.11(b). fault cleared at 120 ms (with proposed controller)

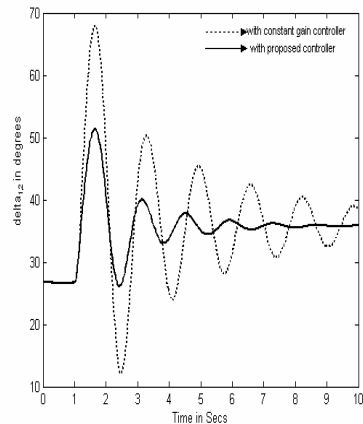


Fig.12. Higher operating condition (fault cleared at 100ms)

6. CONCLUSIONS

This paper has proposed an approach using ANFIS based UPFC for the suppression of small signal oscillations in the power system. The adaptive controller, adapted by a proper training data, is showing improved performance with the four choices of UPFC control signals compared to constant gain controller designed at a nominal operating condition. This makes the real time implementation flexible with respect to the choice of control

signal. With regard to damping of low frequency oscillations of the system, it is observed that the performance of the proposed controller is improving when the UPFC is installed with control signals based on phase angle modulation of shunt and series converter voltages, which results in real power exchange with respect to the system. Investigations also illustrate the superiority of the proposed controller under large disturbance when compared to the constant gain controller. Further investigations are under progress to take care of the possible negative interactions between the various control channels of UPFC, when UPFC is installed with different control assignments and also with other power swing damping devices.

References

- [1] Kundur,P.,Klein,M.,Roger,G.J., and Zywno,M.S.: 'Application of power system stabilizers for enhancement of overall system stability', IEEE Trans.on Power System,4,(2),1989, pp.614 - 626.
- [2] Hingorani,N.G.: 'Power Electronics in Electrical Utilities',IEEE Proc.,76,(4),1988,pp.481-482.
- [3] Gyugyi, L., and Schauder et al., C.D.: 'The unified power flow controller: A New Approach to Power Transmission Control', IEEE Trans. on Power Delivery, 10, (2),1995,pp.1085 – 1097.
- [4] Chang,C.T.,Hsu,Y.Y.: 'Design of upfc controllers and supplementary damping controller for power transmission control and stability enhancement of a longitudinal power system', IEE Proc.Gener. Transm.Distrib. 149,2002, pp.463 – 471.
- [5] Tambey,N.,and Kothari,M.L.: 'Upfc based damping controllers for damping low frequency oscillations in a power system', IE(I)journal-EL, 84, 2003, pp. 35-41.
- [6] Tambey,N., and Kothari,M.L. : 'Damping of power system oscillations with unified power flow controller(UPFC)',IEEProc.Gener.Transm.Distrib.,150,(2), 2003, pp.129-140
- [7] Jyh-Shing Roger Jang.: 'ANFIS: Adaptive-Network-Based Fuzzy Inference System', IEEE Trans. Syst. Man and Cyber., 23, (3), 1993,pp. 665-685
- [8] E.V. Larsen, Juan.J, Sanchez-Gasca and Chow.J.H. 'Concept for design of FACTS controllers to damp power swings', IEEE Transactions 1995,PWRS-2 (10), pp.948-956.
- [9] Wang,H.F.: 'Damping function of unified power flow controller', IEE Proc. Gener. Transm. Distrib., 1999, 146, (1), pp.81 - 87.
- [10] Wang,H.F.,Li,M., and Swift,F.J.: 'FACTS –based stabilizer designed by the phase compensation method.Part I and Part II'.Proc. ,APSCOM-97,HongKong,1997,pp.638-649.
- [11] Navabi-Niaki,A.,and Irvani,M.R. : 'Steady –state and dynamic models of UPFC for power system studies',IEEE Transaction on PWRS.,1996,11,(4),pp.1937-1943.
- [12] Wang,H.F.: 'Applications of modeling UPFC into multi-machine power systems', IEE Proc. Gener. Transm. Distrib., 1999, 146, (3), pp.306 - 312.
- [13] IEEE Std 421.5: 'IEEE Recommended Practice for Excitation System Models for Power System stability Studies',1992
- [14] Takagi, T.,and Sugeno, M.: ' Fuzzy identification of systems and its applications to modeling and control',IEEE Trans. Sys. Man and Cyber., 1985,15, pp.116-132.

Appendix 1.SMIB system

Synchronous Machine :

$H=4.0$ s, $D=0.0$, $T_{do}=5.044$ s, $X_d=1.0$ p.u., $X'_d=0.3$ p.u., $X_q=0.6$ p.u

Excitation system: $K_a=100$, $T_a=0.01$ s

Transformer and Transmission line

$X_{TE}=0.1$ p.u., $X_E=0.1$ p.u., $X_B=0.1$ p.u., $X_{Bv}=0.3$ p.u., $X_e=0.5$ p.u

Nominal operating condition:

$P_e=0.8$ p.u., $Q_e=0.2$ p.u., $V_t=1.0$ p.u., $f=60$ Hz

UPFC parameters

$m_E=0.4$, $m_B=0.08$, $\delta_E=-85.3^\circ$, $\delta_B=-78.2^\circ$, $V_{dc}=2$ p.u., $C_{dc}=1$ p.u

K constants calculated for the nominal operating conditions:

$k_1=0.5661$, $k_2=0.1712$, $k_3=2.4583$, $k_4=0.4198$,

$k_5=-0.1513$, $k_6=0.3516$, $k_7=0.0906$, $k_8=0.0457$,

$k_9=0.0016$ $k_{pd}=0.0835$, $k_{vd}=-0.0964$, $k_{qd}=0.2446$

$k_{pe}=0.3795$, $k_{pb}=0.1864$, $k_{p\delta e}=1.1936$, $k_{p\delta b}=0.0529$

$k_{qe}=1.1628$, $k_{qb}=0.2855$, $k_{q\delta e}=-0.0380$, $k_{p\delta b}=-0.0423$

$k_{ve}=-0.4591$, $k_{vb}=-0.1096$, $k_{v\delta e}=0.0311$, $k_{v\delta b}=0.0189$

$k_{ce}=-0.0192$, $k_{cb}=0.0991$, $k_{c\delta e}=-2.0312$, $k_{c\delta b}=0.0793$

Appendix.2.(A). 3-Machine system (System MVA base=100)

Synchronous Machines :

$H_1=20.09$ s., $H_2=H_3=11.8$ s., $D_1=D_2=D_3=0$, $T'_{d01}=7.5$ s., $T'_{d02}=T'_{d03}=4.7$ s.

$X_{d1}=0.19$ p.u., $X_{d2}=X_{d3}=0.42$ p.u., $X'_{d1}=0.08$ p.u., $X'_{d2}=X'_{d3}=0.173$ p.u.,

$X_{q1}=0.16$ p.u., $X_{q2}=X_{q3}=0.32$ p.u.

Excitation system:

$K_{a1}=20$, $K_{a2}=K_{a3}=100$, $T_{a1}=0.05$ s., $T_{a2}=T_{a3}=0.01$ s.,

PSS parameters:

$K_{pss2}=3$, $T_1=0.3$ s., $T_2=0.15$ s., $K_{pss3}=4$, $T_1=0.2$ s., $T_2=0.05$ s.,

Nominal operating condition:

$P_{e1}=0.714$ p.u., $P_{e2}=1.63$ p.u., $P_{e3}=0.853$ p.u., $V_{T1}=1.04$ p.u., $V_{T2}=1.025$ p.u., $V_{T3}=1.025$ p.u.

Higher operating condition:

$P_{e1}=2.2074$ p.u., $P_{e2}=1.92$ p.u., $P_{e3}=1.28$ p.u., $V_{T1}=1.04$ p.u., $V_{T2}=1.025$ p.u., $V_{T3}=1.025$ p.u.

(B). UPFC parameters

Series converter rating = 1.78 p.u., Shunt converter rating = 0.6 p.u.

$X_B=0.0135$ p.u., $X_E=0.036$ p.u.

Initial UPFC series and shunt source voltages:

$V_B=0.1108 \angle -97.8^\circ$ $V_E=0.974 \angle 3^\circ$

Damping controller parameters:

$K_s=2$, $T_w=0.1$ s., $T_3=0.2$ s., $T_3=0.34$ s.